Goodput and Delay Cross-Layer Analysis of IEEE 802.11a Networks with Link Level Tecnhiques over Block Fading Channels

Roger Pierre Fabris Hoefel

***Resumo* — Neste artigo é desenvolvido e validado um modelo teórico que permite estimar a taxa liquida em bits por segundo e o atraso médio em redes locais IEEE 802.11a. Estes resultados teóricos são empregados para analisar comparativamente o desempenho de redes 802.11a em canais com desvanecimento independente e com desvanecimento correlacionado.**

***Palavras-Chave*—Redes locais sem fio, 802.11a, protocolos de controle de acesso ao meio, eficiência, atraso, desvanecimento.**

***Abstract* — It is developed a theoretical cross-layer model that allows assessing the goodput and delay of the IEEE 802.11a local area networks (WLANs) operating under saturated traffic conditions. This model takes into account the distributed coordination function (DCF) request-to-send/clear-to-send (RTS/CTS) medium access control (MAC) protocol, the physical (PHY) layer and an adaptive link level scheme.**

***Index Terms*—WLANs, 802.11a, MAC protocols, throughput, goodput, delay, multipath fading.**

I. INTRODUCTION

In [1], we developed a theoretical cross-layer model for MAC and PHY layer protocols for networks based on the IEEE 802.11 standard. The analytical expressions derived allow estimate the effects of distinct modulation schemes, channel models and an adaptive link level scheme on the system performance. However, in [1] the MAC 802.11 contention window (CW) resolution algorithm was not implemented (i.e. the packets are dropped after the first non-successful transmission attempted) in order that the simulated offered traffic follows strictly the Poisson statistics, as analytically postulated.

Based on the methodology proposed by Bianchi in [2], we have developed a cross-layer saturation goodput theoretical model for IEEE 802.11a WLANs for the DCF basic access scheme [3] and RTS/CTS access mechanism [4] MAC protocols that takes into account the effects of backoff scheme and non-ideal channel conditions. The models developed in [3] and [4] allow assessing the system performance over an uncorrelated Rayleigh fading channel (i.e. a fading channel temporally independent at symbol level and independent across orthogonal frequency division modulation (OFDM) carriers).

In the present contribution we improve our previous theoretical results by: *(1)* developing a cross-layer theoretical model that allows estimate the goodput and delay of IEEE 802.11a WLANs over correlated fading channels; *(2)* carrying out a comparison between the performance of IEEE 802.11a over uncorrelated and correlated fading channels; *(3)* investigating the improvements due to an adaptive modulation and coding scheme suited to 802.11a standard. The above contributions are developed in Sections V to VIII. Therefore, the next three sections, a necessary background to the reader not familiarized with this technology, are included to present fundamental aspects regarding to 802.11a MAC (Section II) and PHY (Section III) layers as well as to summarize some of our earlier theoretical results (Section IV).

Roger Pierre Fabris Hoefel, Department of Telecommunications Engineering, University La Salle (UNILASALLE), Canoas, Rio Grande do Sul, Brazil, E-mail: roger@lasalle.tche.br

II. IEEE 802.11 RTS/CTS MAC

Fig. 1 shows the time diagram for the atomic transmission used by the DCF RTS/CTS mechanism [5]. The virtual carrier-sending is implemented by the network allocation vector (NAV), which is a timer updated by a control field transmitted in data and control frames in order to set the amount of time that the channel will be reserved to permit uninterrupted atomic transmissions. If the NAV is zero, then the station (STA) implements a channel sensing procedure, so that the transmission can begin immediately if the channel has been idle for longer than the DCF interframe spacing (DIFS). If the channel is busy, the station must backoff its transmission until the channel becomes idle for the DIFS period. After this DIFS period, the station: *(1)* it starts to treat the channel in units of time slot; *(2)* it implements a binary exponential backoff period (EBP) to determine the time slot access time; *(3)* it continues to check the channel to verify if it is busy or idle; *(4)* it decrements the EBP while the channel is idle. If the channel remains idle when the EBP becomes zero, then the STA starts its MAC protocol data unit (MPDU) transmission. Otherwise, the decrement of backoff interval stops and only resumes after the channel is detected idle for the DIFS period. If the RTS frame transmission is successful, the peer STA sends a CTS control frame to confirm the reservation. After that, it is transmitted a data unicast frame. The sender STA must use the extended interframe spacing (EIFS) to set the time for new physical channel sensing if either data or control frames are corrupted or due to the timeout of timer that controls the maximum expected delay of the CTS control frame.

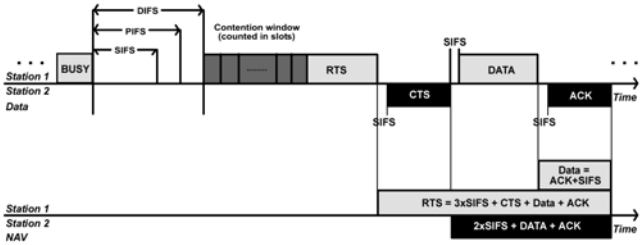

Fig. 1. The clearing technique used at atomic RTS/CTS scheme.

III. IEEE 802.11 PHYSICAL LAYER

The IEEE 802.11a is based on OFDM using a total of 52 subcarriers, of which 48 subcarriers carry actual data and four

subcarriers are pilots used to facilitate coherent detection [6]. The channel symbol rate R_s is of *12 Msymbols/sec* since the OFDM symbol interval, *tS* is set to 4μs. Tab. 1 shows the OFDM PHY modes, where *BpS* means Bytes per Symbol.

TABLE I
The IEEE 802.11a PHY modes [7].

Mode p	*Modulation*	*Code Rate R_c*	*Data Rate*	*BpS*
1	BPSK	1/2	6 Mbps	3
2	BPSK	3/4	9 Mbps	4.5
3	QPSK	1/2	12 Mbps	6
4	QPSK	3/4	18 Mbps	9
5	16-QAM	1/2	24 Mbps	12
6	16-QAM	3/4	36 Mbps	18
7	64-QAM	2/3	48 Mbps	24
8	64-QAM	3/4	54 Mbps	27

Considering the IEEE 802.11a generator polynomials, $\boldsymbol{g_0}=(133)_8$ and $\boldsymbol{g_1}=(171)_8$, of rate $r=1/2$ and constrain length $K=7$ [6, pp.16], then the union bound on the probability of decoding error is given by [8]

$$P_e(\gamma_b,p) < 11P_{10}(\gamma_b,p)+38P_{12}(\gamma_b,p)+193P_{14}(\gamma_b,p)+\cdots, \quad (1)$$

where the notation emphasizes the dependence of P_d with the received signal-to-interference-plus-noise (SINR) per bit γ_b, and the *PHY mode p*.

The union bound on the probability of decoding error for the higher code rates of 2/3 and 3/4 (which are obtained by puncturing the original rate-1/2 code [6]), are given by (2) and (3), respectively [9].

$$P_e(\gamma_b,p) < P_6(\gamma_b,p)+16P_7(\gamma_b,p)+48P_8(\gamma_b,p)+\cdots, \quad (2)$$

$$P_e(\gamma_b,p) < 8P_5(\gamma_b,p)+31P_6(\gamma_b,p)+160P_7(\gamma_b,p)+\cdots, \quad (3)$$

Assuming that the convolutional forward error correcting code (FEC) is decoded using hard-decision Viterbi decoding, then (4) and (5) model the probability of incorrectly selecting a path when a the Hamming distance *d* is even and odd, respectively. The average bit error rate (BER) for the *PHY mode m* modulation scheme is denoted by ρ_p.

$$P_d(\gamma_b,p)=\frac{1}{2}\binom{d}{d/2}p_p^{d/2}(1-\rho_p)^{d/2}+\sum_{k=d/2+1}^{d}\binom{d}{k}\rho_p^k(1-\rho_p)^{d-k}. \quad (4)$$

$$P_d(\gamma_b,p)=\sum_{k=(d+1)/2}^{d}\binom{d}{k}\rho_p^k(1-\rho_p)^{d-k}. \quad (5)$$

The RTS and CTS control frames must be transmitted at one of the rates of the basic service set (BSS) so that they can be decoded by all the STAs in the same network. The mandatory BSS basic rate set is {6 Mbps, 12 Mbps, 24 Mbps}. The ACK control frame must be transmitted using the BSS basic rate that is less than or equal to the rate of the data frame it is acknowledging.

The MPDU, RTS, CTS and ACK frames are encapsulated into the physical layer PDU (PPDU) as shown at Fig. 2.

The physical layer convergence procedure (PLCP) preamble duration, *tPCLP_Pre*, is equal to 16 μs. The PCLP header is always transmitted using PHY 1 and its duration, *tPCLP_SIG*, is equal to 4 μs. The *SERVICE* field has 16 bits and 6 tail bits are used to flush the convolutional code to the "zero state".

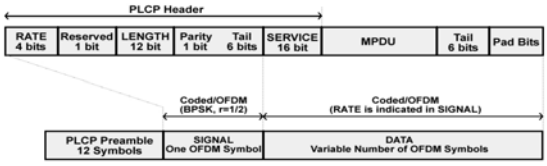

Figure 2. PPDU frame format of the IEEE 802.11a [6, pp.7].

The number of octets of the PPDU that transport the RTS frame is given by

$$N_{rts}=N_{pre}+N_{srv}+l_{rts}+N_{tail}=3+\frac{16}{8}+20+\frac{6}{8}, \quad (6)$$

where N_{pre}, N_{srv} and N_{tail} denote the number of octets of the preamble, service and tail fields, respectively. The numbers of octets used to carry the "logical control information" send by the RTS frame is denoted by l_{rts}.

The number of octets of the PPDU that transport the CTS and ACK control frame is given by

$$N_{cts}=N_{ack}=N_{pre}+N_{srv}+l_{cts}+N_{tail}=3+\frac{16}{8}+14+\frac{6}{8}, \quad (7)$$

where $l=l_{cts}=l_{ack}=14$ *octets*.

The MAC PPDU length is given by

$$N_{mp}=N_{pre}+N_{srv}+N_{mh}+N_{pl}+N_{tail}=3+\frac{16}{8}+34+N_{pl}+\frac{6}{8}, \quad (8)$$

where the MPDU header and the cyclic redundant checking (CRC) fields have together a length of 34 bytes [5, pp. 52].

The duration of RTS, CTS and ACK control frames are given by (9-11), respectively.

$$T_{rts}(p_{rts})=tPCLP\_Pre+tPCLP\_SIG+\left\lceil\frac{l_{rts}+(16+6)/8}{BpS(p_{rts})}\right\rceil\cdot tS. \quad (9)$$

$$T_{cts}(p_{cts})=tPCLP\_Pre+tPCLP\_SIG+\left\lceil\frac{l_{cts}+(16+6)/8}{BpS(p_{cts})}\right\rceil\cdot tS. \quad (10)$$

$$T_{ack}(p_{ack})=tPCLP\_Pre+tPCLP\_SIG+\left\lceil\frac{l_{ack}+(16+6)/8}{BpS(p_{ack})}\right\rceil\cdot tS. \quad (11)$$

The transmission period to transmit a MPDU with a payload of N_{pl} *octets* over the IEEE 802.11a using the *PHY mode p* is given by

$$T_{mp}(p_{mp})=tPCLP\_Pre+tPCLP\_SIG+\left\lceil\frac{N_{pl}+34+(16+6)/8}{BpS(p_{mp})}\right\rceil\cdot tS. \quad (12)$$

IV. GOODPUT: ANALYTICAL RESULTS

A. Packet Transmission Probability

Here, we show the main steps regarding the derivation of the goodput theoretical model for the IEEE 802.11a RTS/CTS MAC protocol. The reader is referenced to [4] in order to get the full mathematical details. It is assumed a fixed number of *n* STAs operating in saturation conditions, i.e. each STA has a packet to transmit after the completion of each successful transmission.

Fig. 3 shows a discrete Markov chain for the backoff window size assuming the MAC RTS/CTS mechanism, where *s(t)* is the stochastic process of the backoff stage *(0, ···,m)* of the STA at time *t* and *b(t)* is the random process that models the backoff time counter for a given STA. This model assumes that each packet collides with a constant and independent

conditional collision probability p. The window size at backoff stage *i* is labeled as $W_i = 2^i W$, where $i \in (0,m)$ is the backoff stage and W is the MAC CW size parameter CW_{min} The maximum window size is denoted as $W_m = 2^m W - 1 = CW_{max}-1$.

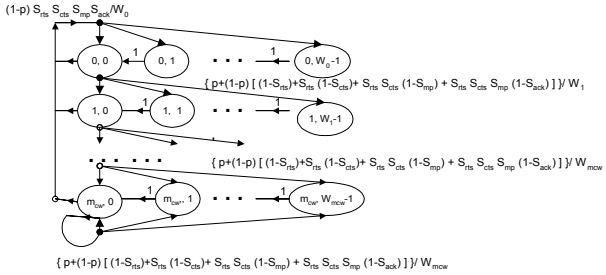

Figure 3. Bi-dimensional Markov chain *(s(t),b(t))* model for the IEEE 802.11 backoff window size and a non-ideal channel assumption. $W_i = 2^i W$.

Using the short notation $P\{i_1,k_1/i_0,k_0\}=P\{s(t+1)=i_1,b(t+1)=k_1 | s(t)=i_0,b(t)=k_0\}$, (13) to (16) model the null one-step transition probabilities of the Markov chain depicted at Fig. 3.

$$P\{i,k \mid i,k+1\}=1 \quad for\ k\in(0,W_i-2)\ and\ i\in(0,m). \tag{13}$$

$$P\{0,k \mid i,0\}=(1-p)\cdot S_{rts}\cdot S_{cts}\cdot S_{mp}\cdot S_{ack}/W_0 \quad for\ k\in(0,W_0-1)\ and\ i\in(0,m) \tag{14}$$

$$P\{i,k \mid i-1,0\}=\{p+(1-p)\cdot(1-S_{rts}\cdot S_{cts}\cdot S_{mp}\cdot S_{ack})\}/W_1 \quad for\ k\in(0,W_i)\ \text{and}\ i\in(1,m). \tag{15}$$

$$P\{m,k \mid m,0\}=\{p+(1-p)\cdot(1-S_{rts}\cdot S_{cts}\cdot S_{mp}\cdot S_{ack})\}/W_m \quad k\in(0,W_m-1). \tag{16}$$

Eq. (13) models the decreasing of the backoff timer at the beginning at each slot time of size σ.

Eq. (14) takes into account that a new physical layer convergence procedure (PCLP) protocol data unit (PPDU) starts at backoff stage 0 and that the backoff is uniformly distributed into the range *(0, W_0-1)* after a successful PPDU transmission. S_{cts}, S_{rts} and S_{ack} denote, respectively, the probability that the RTS, CTS and ACK control frames be transmitted with success. S_{mp} denotes the probability the transmission of a MPDU (i.e. a MAC PDU) is successful.

Eq. (15) models the fact that a new backoff value is uniformly chosen in the range *(0,W_i)* after an unsuccessful transmission at the backoff stage *i-1*. The capture effect is neglected in such way that the lost of frames due to collisions is independent of the lost of frames due to noise and interference.

Eq. (16) models the property that the backoff is not increased in subsequent frame transmissions once the backoff stage has reached the value *m*.

Any transmission occurs when the backoff timer counter is equal to zero, then it can be shown that the probability that a STA transmits in a randomly chosen slot time is

$$\tau=\sum_{i=0}^{m} b_{i,0}=\frac{b_{0,0}}{S\cdot(1-p)}=\frac{b_{0,0}}{S_{rts}\cdot S_{cts}\cdot S_{mp}\cdot S_{ack}\cdot(1-p)}, \tag{17}$$

where

$$b_{0,0}=\frac{2\cdot(1-p)\cdot S\cdot[1+2\cdot S\cdot(p-1)]}{1+2^m W\cdot[1+(-1+p)\cdot S]^m+(-1+p)\cdot S\cdot\{2+W+2^m W\cdot[1+(-1+p)\cdot S]^m\}}. \tag{18}$$

Each STA transmits with probability *τ*. Therefore, postulating that a given STA is transmitting, the probability that a transmitted PPDU encounters a collision in a given slot time can be stated as

$$p=1-(1-\tau)^{n-1}, \tag{19}$$

The nonlinear system represented by (17) and (19) can be solved using numerical techniques.

B. Goodput

The goodput (or net throughput) in *bits per second (bps)* can be defined as the probability that a MAC payload with N_{pl} *octets* be transmitted with success in the average cycle time $\overline{T}$, i.e.

$$G_{bps}(m)=\frac{8\cdot N_{pl}\cdot P_s\cdot P_{tr}\cdot S_{rts}\cdot S_{cts}\cdot S_{mp}\cdot S_{ack}}{\overline{T}}. \tag{20}$$

The probability that there is no collision on the channel conditioned to the fact that at least one STA transmits is given by

$$P_s=\frac{n\cdot\tau\cdot(1-\tau)^{n-1}}{P_{tr}}=\frac{n\cdot\tau\cdot(1-\tau)^{n-1}}{1-(1-\tau)^n}, \tag{21}$$

where P_{tr} is the probability that there is at least one transmission that occurs in the considered slot time.

The average cycle time is given by

$$\overline{T}=\overline{B}_S+\overline{B}_{f1}+\overline{B}_{f2}+\overline{B}_{f3}+B_{f4}+B_{f5}+\overline{I}. \tag{22}$$

The average busy time for a successful transmission is given by:

$$\overline{B}_S=P_s\cdot P_{tr}\cdot S_{rts}\cdot S_{cts}\cdot S_{mp}\cdot S_{ack}\cdot\left[DIFS+T_{rts}(p_{rts})+a+SIFS+T_{cts}(p_{cts})+a+SIFS+T_{mp}(p_{mp})+a+SIFS+T_{ack}(p_{ack})+a\right] \tag{23}$$

where *a* is the propagation delay. $T_{rts}(p_{rts})$, $T_{cts}(p_{cts})$ and $T_{ack}(p_{ack})$ denote the time necessary to transmit the RTS, CTS and ACK frames when it is used the *PHY mode* p_{rts}, p_{cts} and p_{ack}, respectively. $T_{mp}(p_{mp})$ is the time necessary to transmit a MPDU payload for the *PHY mode* p_{mp}.

$\overline{B}_{f1}$ models the average amount of time in which the channel is busy due to collisions at the transmission of RTS control frames. $\overline{B}_{f2}$, $\overline{B}_{f3}$, $\overline{B}_{f4}$ and $\overline{B}_{f5}$ model the average time that the channel is busy with unsuccessful transmissions, due to noise and interference, of RTS, CTS, MPDU and ACK frames, respectively.

$$\overline{B}_{f1}=P_{tr}\cdot(1-P_S)\cdot\left[EIFS+T_{rts}(p_{rts})+a\right]. \tag{24}$$

$$\overline{B}_{f2}=P_{tr}\cdot P_s\cdot(1-S_{rts})\ \left[EIFS+T_{rts}(p_{rts})+a\right]. \tag{25}$$

$$\overline{B}_{f3}=P_{tr}\cdot P_s\cdot S_{rts}\cdot(1-S_{cts})\left[EIFS+T_{rts}(p_{rts})+a+SIFS+T_{cts}(p_{cts})+a\right] \tag{26}$$

$$\overline{B}_{f4}=P_{tr}\cdot P_s\cdot S_{rts}\cdot S_{cts}\cdot(1-S_{mp})\left[EIFS+T_{rts}(p_{rts})+a+SIFS+T_{cts}(p_{cts})+a+SIFS+T_{mp}(p_{mp})+a\right]. \tag{27}$$

$$\overline{B}_{f5}=P_{tr}\cdot P_s\cdot S_{rts}\cdot S_{cts}\cdot S_{mp}\cdot(1-S_{ack})\left[EIFS+T_{rts}(p_{rts})+a+SIFS+T_{rcs}(p_{cts})+a+SIFS+T_{mp}(p_{mp})+a+SIFS+T_{ack}(p_{ack})+a\right]. \tag{28}$$

The average time that a slot is idle is given by

$$\overline{I}=(1-P_{tr})\cdot\sigma. \tag{29}$$

V. DELAY: ANALYTICAL RESULTS

The average delay between the time that a MPDU arrived at the queue until the time that an ACK for this MPDU is received can be modeled as

$$\overline{D} = \overline{\mathrm{P}} \cdot \left(\overline{B}_s + \overline{B}_{f1} + \overline{B}_{f2} + \overline{B}_{f3} + \overline{B}_{f4} + \overline{B}_{f5} + \overline{I} \right), \quad (30)$$

where the average number of slot times spend for a successful transmission is given by

$$\overline{P} = \sum_{i=0}^{m-1} \left[\left(P_f\right)^i \frac{W_i}{2} \right] + \sum_{i=m}^{\infty} \left[\left(P_f\right)^i . \frac{W_m}{2} \right]. \quad (31)$$

The probability that a transmission is corrupted is given by

$$\begin{aligned} P_f &= p + (1-p) \cdot \begin{bmatrix} (1 - S_{rts}) + S_{rts}(1 - S_{cts}) + S_{rts} \cdot S_{cts} \cdot (1 - S_{mp}) + \\ S_{rts} \cdot S_{cts} \cdot S_{mp} \cdot (1 - S_{ack}) + \end{bmatrix} \\ &= p + (1-p) \cdot \left(1 - S_{rts} \cdot S_{cts} \cdot S_{mp} \cdot S_{ack}\right), \end{aligned} \quad (32)$$

where the collision probability p is obtained resolving the nonlinear system represented by (17) and (19)

VI. ANALYTICAL RESULTS FOR FRAME SUCCESS PROBABILITY OVER BLOCK CORRELATED FADING CHANNELS

Assuming that the errors inside of the decoder are interdependent, then *Pursley* and *Taipale* have shown that the upper bound for a successful transmission of a frame with l octets is given by [10]

$$S(l, \gamma_b, p) < \left[1 - P_e(\gamma_b, p)\right]^{8l} \quad (33)$$

For a block-fading channel, this upper bound may be modify to

$$S(l, \gamma_b, p) < \int_{\gamma_{\inf}}^{\infty} [1 - Pe(\gamma_b, p)]^{8l} \, p(\gamma_b) d\gamma_b \quad (34)$$

where the $P_m(\gamma_b)$ is a function that depends on γ_b and the *PHY mode p.* The lower limit of the definite integral is chosen such as $[1 - Pe(\gamma_b, m)]^{8l} \le 1$ for $\gamma_b \ge \gamma_{\inf.}$.

Considering a Nakagami-m fading channel, a maximum ratio combining (MRC) receiver matched with the channel diversity and that the same average power Ω is received at each diversity branch, then the probability distribution function (pdf) of the SINR per bit at the Viterbi decoder input is of gamma kind [11], i.e.

$$p(\gamma_b) = \frac{1}{\Gamma(L\, m_n)} \left(\frac{m_n}{\bar{\gamma}_b} \right)^{L\, m_n} (\gamma_b)^{L\, m_n - 1} \exp\left(- \frac{m_n\, \gamma_b}{\bar{\gamma}_b} \right) \quad if \;\; \gamma_b > 0, \; m_n \ge 0.5, \quad (35)$$

where m_n is the Nakagami-m fading figure, $\bar{\gamma}_b$ is the average SINR per bit at the detector output (or at Viterbi decoder input) and L is the number of receiver diversity branches.

1. PHY Mode 1 (BPSK@6Mbps)

For the PHY mode 1 $P_m(\gamma_b)$ is given by (4) with ρ_p given by

$$P_p(\gamma_b) = Q\left(\sqrt{2\gamma_b R_c}\right), \quad (36)$$

where γ_b is the SINR per bit, R_c is the code rate and $Q(x)$ is the complementary Gaussian cumulative distribution function [12].

Since all frames are transmitted using the *PHY mode 1*, then S_{rts}, S_{cts}, S_{mp} *and* S_{ack} can be estimated using (37-43) with $p=1$.

$$S_{rts}(p) = S(N_{rts}, \gamma_b, p) \; . \quad (37)$$

$$S_{cts}(p) = P\{CTS \;\; is \;\; correct \;/\; RTS \;\; was \;\; correct\}; \quad (38)$$

$$S_{cts}(p) = \frac{S(N_{rts} + N_{cts}, \gamma_b, p)}{S_{rts}}. \quad (39)$$

$$S_{mp}(p) = P\{MPDU \; is \; correct \;/\; RTS \; and \; CTS \; were \; correct\}; \quad (40)$$

$$S_{mp}(p) = \frac{S(N_{rts} + N_{cts} + N_{mpd}, \gamma_b, p)}{S_{rts} S_{cts}} . \quad (41)$$

$$S_{ack}(p) = P\{ACK \; is \; correct / \; RTS, CTS \; and \; MPDU \; were \; correct\}; \quad (42)$$

$$S_{ack}(p) = \frac{S(N_{rts} + N_{cts} + N_{mpd} + N_{ack}, \gamma_b, p)}{S_{rts} S_{cts} S_{mpd}} . \quad (43)$$

2. PHY Mode 2 (BPSK@9Mbps)

In this case all the control frames are transmitted using the PHY mode 1 and the MPDU is transmitted using the PHY 2. Thus, the S_{rts} and S_{cts} are still given by (37) and (39) with $p=1$. The S_{md} is given by

$$S_{mpd}(2) \cong \frac{S(36.75 + N_{mpd}, \gamma_b, 2)}{S_{rts}(1) S_{cts}(1)} = \frac{S(36.75 + N_{mpd}, \gamma_b, 2)}{S(N_{rts} + N_{cts}, \gamma_b, 1)} . \quad (44)$$

Notice that the 3 octets of the preamble were not taken into account in (43) since they are transmitted using the PHY mode 1. We also use the following approximation

$$\begin{aligned} P\{MPDU \; is \; ack \;/\; RTS \; and \; CTS \; were \; ack\} &= \frac{P\{MPDU, RTS, CTS\}}{P\{RTS, CTS\}} \\ &\approx \frac{P\{MPDU\}}{P\{RTS, CTS\}} \end{aligned} \quad (45)$$

since $N_{mp} >> (N_{rts} + N_{cts})$ and the MPDU is transmitted using the PHY mode 2 (i.e. a signaling scheme with less immunity to noise and interference than the signaling scheme used to transmit the control frames).

The ACK control frame is transmitted using the PHY mode 1, while the MPDU is transmitted using the PHY mode 2 (i.e. a signaling scheme more suitable to decoding errors). Thus, the ACK control frame success probability can be approximated by (46) for a block fading channel.

$$S_{ack}(p) = P\{ACK \;\; is \;\; ack \;/\; RTS, CTS \; and \; MPDU \;\; were \;\; ack) \cong 1. \quad (46)$$

3. PHY Mode 3(QPSK@12Mbps)

In this case all control and data frames are all transmitted using the PHY mode 3. Therefore, S_{rts} and S_{cts} are given by (37) and (39), respectively, with $p=3$. Correspondingly, S_{md} and S_{ack} are given by (41) and (43) with p=3. Notice that $P_p(\gamma_b)$ is still given by (36) for coherent demodulation [12].

4. PHY Mode 4 (QPSK@18Mbps)

Here, all the control frames are transmitted using the PHY mode 3 and the MPDU is transmitted using the PHY 4. Consequently, S_{rts} and S_{cts} are given by (37) and (39), respectively, with $p=3$. Using similar reasoning developed for PHY mode 2, then it is easy to verify that S_{md} is given by

$$S_{mpd}(4) \cong \frac{S(36.75 + N_{mpd}, \gamma_b, 4)}{S_{rts}(3) S_{cts}(3)} = \frac{S(36.75 + N_{mpd}, \gamma_b, 4)}{S(N_{rts} + N_{cts}, \gamma_b, 3)}, \quad (47)$$

and that S_{ack} is given by (46).

5. PHY Mode 5 (16QAM@24Mbps)

In this case all control and data frames are all transmitted using the PHY mode 5. Therefore, S_{rts} and S_{cts} are given by (37) and (39), respectively, with $p=5$. Correspondingly, S_{md} and S_{ack} are given by (41) and (43) with $p=5$.
$P_p(\gamma_b)$ for QAM signaling is given by [13]

$$P_p(\gamma_b) = \frac{\sqrt{M}-1}{\sqrt{M}\log_2\sqrt{M}} erfc\left(\sqrt{\frac{2\log_2 M \cdot \gamma_b \cdot R_c}{2(M-1)}}\right) + \frac{\sqrt{M}-2}{\sqrt{M}\log_2\sqrt{M}} erfc\left(\sqrt{\frac{3\log_2 M \cdot \gamma_b \cdot R_c}{2(M-1)}}\right), \quad (48)$$

where erfc(z) is the complementary error function and *p=5,6, 7 and 8*

6. PHY Mode 6 (16QAM@36Mbps), PHY Mode 7 (64QAM@48Mbps) and PHY Mode 8(64QAM@64Mbps)

In this case all the control frames are transmitted using the PHY mode 5 and the MPDU is transmitted using the PHY 6, 7 or 8. Thus, the S_{rts} and S_{cts} are again given by (37) and (39) with $p=5$.
The S_{md} is given by

$$S_{mpd}(p) \cong \frac{S(36.75 + N_{mpd}, \gamma_b, p)}{S_{rts}(5) S_{cts}(5)} = \frac{S(36.75 + N_{mpd}, \gamma_b, p)}{S(N_{rts} + N_{cts}, \gamma_b, 5)} \quad (49)$$

where $p= 6,7$ *and* 8. Notice that we used the approximation (45) since the control frames are transmitted 16QAM with $R_c=1/2$ while the MPDU is transmitted using 16QAM with $R_c=3/4$, 64QAM with $R_c=2/3$ or 64QAM with $R_c=3/4$.
As we have conclude for the PHY mode 2, S_{ack} is given by (46).

VII. ANALYTICAL AND SIMULATION RESULTS

The simulations results are obtained using a C object oriented IEEE 802.11 joint link level and system level simulator described in [4]. We have assumed the following parameters: *slot time* $\sigma=9\mu S$, *SIFS=16* μs, *DIFS=EIFS=34* μs, $CW_{min}=16$, $CW_{max}=1023$, $m_{cw}=6$, $a=1\mu.s$, $N_{pl}=1023$ *octets.*
Fig. 4 compares the goodput as a function of the SINR per bit for a system without spatial diversity. First, we emphasize the good agreement between analytical and simulation results. Second, we can see that the *PHY mode 3* (QPSK with R_c=1/2) and *PHY mode 4* (QPSK with R_c=3/4) allows, respectively, a superior performance in relation to that one obtained with the *PHY mode 1* (BPSK with R_c=1/2) and *PHY mode 2* (BPSK with R_c=3/4), since the QPSK signalling has a better spectral efficiency when it is implemented coherent demodulation. Finally, we point out that for this channel the goodput is maximized with the following PHY modes: *(a)* PHY 3 (γ_b < 6 dB); *(b)* PHY 4 (6 dB ≤ γ_b < 10 dB); *(c)* PHY 6 (10 dB ≤ γ_b < 18.5 dB); *(d)* PHY 8 (18.5 dB ≤ γ_b).

Fig. 5 compares the goodput as a function of the SINR per bit for a system with L=3 receiving antennas. Notice that for this channel the goodput is maximized with the following PHY modes: *(a)* PHY 3 (γ_b < 2 dB); *(b)* PHY 4 (2 dB ≤ γ_b < 5 dB); *(c)* PHY 5 (5 dB ≤ γ_b < 6.5 dB); *(d)* PHY 6 (6.5 dB ≤ γ_b< 12.2 dB); *(e)* PHY 8 (12.2 dB < γ_b).
Fig. 4 and 5 have shown that for correlated fading channels temporally there is a strong dependence between the PHY mode (i.e. a combination of modulation and coding scheme) that maximize the goodput and the spatial diversity. The interested reader is referenced to [4] in order to find a theoretical investigation on temporally uncorrelated fading channels.

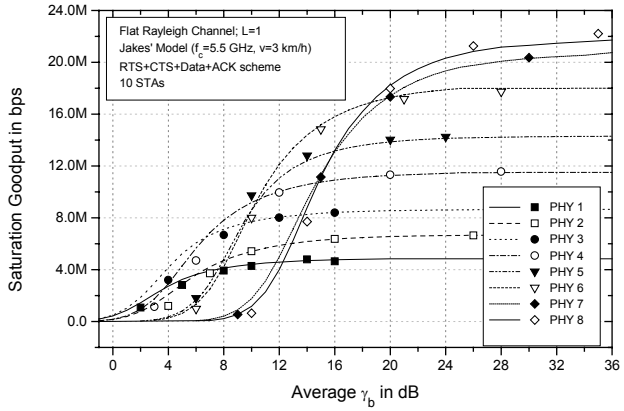

Figure 4. Comparison between analytical (straight lines) and simulation (marks) results for the goodput in bps over a correlated fading channel. L=1.

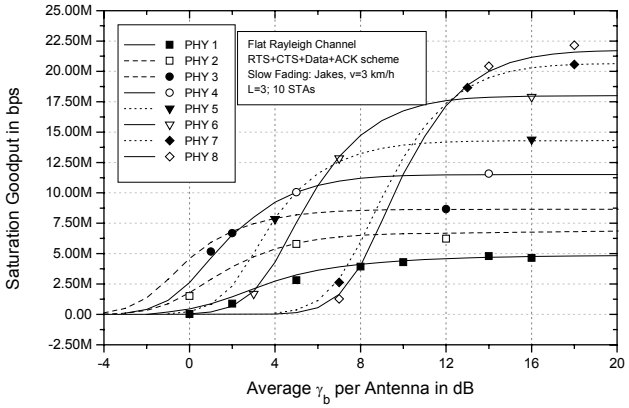

Figure 5. Comparison between analytical (straight lines) and simulation (marks) results for the goodput in bps over a correlated fading channel. L=3.

Fig 6 shows that for temporally uncorrelated fading channel there is a well-defined short range of SINR per bit where the system performance is acceptable. On the other hand, when the fading is strongly correlated there is a wide and smooth variation of the goodput with SINR per bit. Fig. 6 also shows the spatial diversity (assumed uncorrelated) provides greater gain in the required γ_b on environments where the fading is uncorrelated. Although, the diversity gain is also substantial on temporally correlated fading environments.

We must observe that in order to avoid a cumbersome graphic due to the superposition of results in a similar scale, it is only shown at Fig. 6 the system performance for the PHY modes 3 and 8. However, we can confidentially use the analytical expressions developed in this contribution (as well as in [3-4])

in order to produce an extensive analyzes for the different PHY modes.

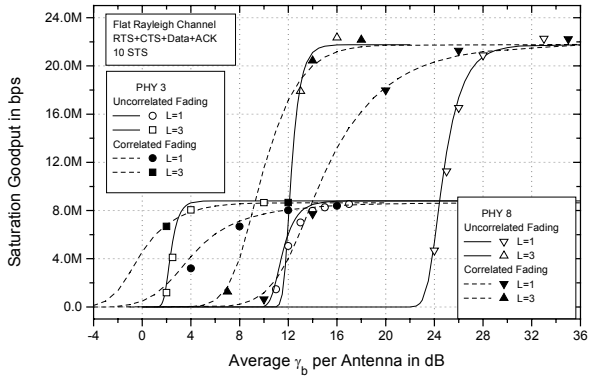

Figure 6. Comparison between analytical (straight lines) and simulation (marks) results for the goodput in bps over a Jakes correlated fading channel and a Rayleigh temporally uncorrelated fading channel.

Finally, Fig. 7 shows a reasonable agreement between numerical and simulation results for the average delay.

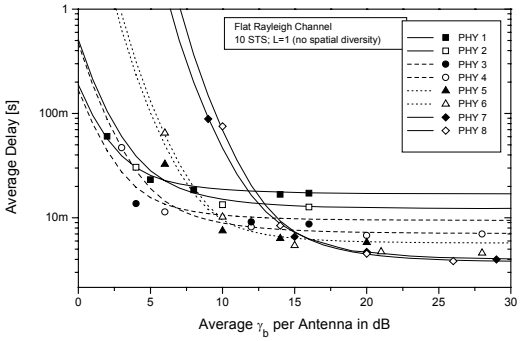

Figure 7. Comparison between analytical (straight lines) and simulation (marks) results for the delay over a correlated fading channel. L=1.

VIII - LINK ADAPTATION

We have investigated the following scheduling scheme:

1. *The received SINR per bit is estimated using the CTS frame;*
2. *If $\gamma_{p-1} \le \gamma_{b,est} < \gamma_p$, then the MPDU is transmitted using the PHY mode p. Here, p belongs to the set of PHY modes that maximize the system performance over the channel model considered. Notice that γ_p denotes the SINR per bit thresholds, which are chosen to maximize the goodput.*

The goodput for the adaptive modulation can be estimated as

$$G_{bps} = \max\left\{G_{bps}(p),\ p = 1,2;\cdots,8\right\}. \quad (50)$$

In the earlier section the control frames are transmitted using the basic service set rate (i.e. PHY modes 1, 3 and 5) that is less than or equal to the rate of the data frame it is acknowledging. Here, the control frames are always transmitted using the PHY mode 1.

Fig. 8 shows analytical and simulation results for a system with adaptive modulation, where the goodput is maximized by dynamically scheduling the PHY mode that maximized the goodput (i.e. the PHY modes 3, 4, 6 and 8). It is also shown results for non-adaptive modulation for *L=1*. We can verify an excellent agreement between analytical and simulation results. Finally, we observe that the set of PHY modes considered depends on the complex interrelations between the modulation scheme, code rate, channel model and so on.

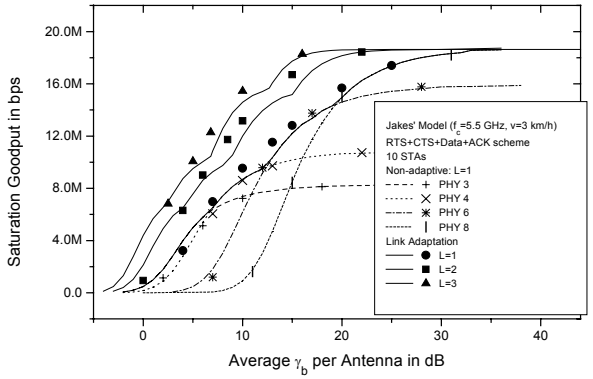

Figure 8. Comparison between analytical (straight lines) and simulation (marks) results for the saturation goodput in bps with an adaptive link scheme (for L=1, 2 and3) and a non-adaptive system (L=1).

IX - FINAL REMARKS

We claim, based on the agreement between simulation and analytical results, that the theoretical results developed in this contribution can be used as an auxiliary toll to analyze and design 802.11a WLANs. As a future research activity on this topic, we shall develop an analytical data link and physical layer model in order to assess the system performance with a limited number of retransmissions for saturated and un-saturated traffic conditions [14].

REFERENCES

[1] R. P. F. Hoefel and C. de Almeida. "Performance of IEEE 802.11-based networks with link level adaptation techniques", *IEEE VTC 2004-Fall*, 2004.

[2] G. Bianchi. "Performance analysis of the IEEE 802.11 distributed coordination function," *IEEE Journal Select. Areas of Commun.,* v.18, no. 3, pp. 535-547, March 2000.

[3] R. P. F. Hoefel. "A Cross-Layer Saturation Goodput Analysis for IEEE 802.11a Networks", *IEEE VTC 2005-Spring*, 2005.

[4] R. P. F. Hoefel. "A Joint MAC and Physical Layer Analytical Model for IEEE 802.11a Networks Operating under RTS/CTS Access Scheme', *Simpósio Brasileiro de Redes de Computadores 2005,* SBRC 2005.

[5] M. S. Gast, *802.11 Wireless Networks*. O'Reilly, 2002.

[6] IEEE 802.11a, Part 11: Wireless LAN Medium Access Control (MAC) and Physical Layer (PHY) Specification – Amendment 1: High-speed Physical Layer in the 5 GHz band". Supplemented to IEEE 802.11 Standard, Sept. 1999.

[7] S. D. Qiao, S. Choi and K. G Shin. "Goodput analyzes and link adaptation for the IEEE 802.11a wireless LANs,*" IEEE Mobile Comp.*, pp. 278-292, 2002.

[8] J Conan. "The weight spectra of some short low-rate convolutional codes," *IEEE Trans. Commun.*, vol. 32, pp. 1050-1053, Sept. 1984.

[9] D. Haccoun and G. Bégin. "High-rate punctured convolutional codes for Viterbi and sequential decoding", *IEEE Trans. Commun*, vol. 37, n.11, pp. 1113-1120, Nov. 1989.

[10] M. B. Pursle and D. J. Taipale. "Error probabilities for spread-spectrum packet radio with convolutional codes and Viterbi decoding", *IEEE Trans. Commun.*, vol. 35, n. 1, p. 1-12, Jan. 1987.

[11] R. P. F. Hoefel and C. de Almeida. "The performance of CDMA/PRMA for Nakagami-m frequency selective fading channel", *Electronics Letters*, vol. 35, no. 1, 1999, pp 28-29.

[12] J. G Proakis, "*Digital Communications",* New York, 2001.

[13] L. Yang and Hanzo, L. "A recursive algorithm for the error probability evaluation of M-QAM," *IEEE Comm. Letters*, vol. 4, pp. 304-306, 2000.

[14] Wu, H.-T et. al. "Performance of reliable transport protocol over IEEE 802.11 wireless LANs: analysis and performance," *INFOCOM 2002,* pp. 599-607, June 2002.